

**Combined ultraviolet- and electron-beam lithography with Micro-Resist-Technology GmbH ma-N1400 resist**

Toen, D.J.; Murugesan, V.; Pascual Laguna, A.; Karatsu, K.; Endo, A.; Baselmans, J.J.A.

**DOI**

[10.1116/6.0001918](https://doi.org/10.1116/6.0001918)

**Publication date**

2022

**Document Version**

Final published version

**Published in**

Journal of Vacuum Science and Technology B

**Citation (APA)**

Toen, D. J., Murugesan, V., Pascual Laguna, A., Karatsu, K., Endo, A., & Baselmans, J. J. A. (2022). Combined ultraviolet- and electron-beam lithography with Micro-Resist-Technology GmbH ma-N1400 resist. *Journal of Vacuum Science and Technology B*, 40(5), Article 052603. <https://doi.org/10.1116/6.0001918>

**Important note**

To cite this publication, please use the final published version (if applicable). Please check the document version above.

**Copyright**

Other than for strictly personal use, it is not permitted to download, forward or distribute the text or part of it, without the consent of the author(s) and/or copyright holder(s), unless the work is under an open content license such as Creative Commons.

**Takedown policy**

Please contact us and provide details if you believe this document breaches copyrights. We will remove access to the work immediately and investigate your claim.

# Combined ultraviolet- and electron-beam lithography with Micro-Resist-Technology GmbH ma-N1400 resist

Cite as: J. Vac. Sci. Technol. B **40**, 052603 (2022); <https://doi.org/10.1116/6.0001918>

Submitted: 15 April 2022 • Accepted: 10 August 2022 • Published Online: 23 September 2022

Published open access through an agreement with Technische Universiteit Delft Afdeling Micro-elektronica

 D. J. Thoen,  V. Murugesan,  A. Pascual Laguna, et al.



View Online



Export Citation



CrossMark

## ARTICLES YOU MAY BE INTERESTED IN

### Molecular appreciation!


The Physics Teacher **60**, 532 (2022); <https://doi.org/10.1119/10.0014296>


### US particle physicists envision future of the field

Physics Today **75**, 22 (2022); <https://doi.org/10.1063/PT.3.5097>

### Aberration control in quantitative widefield quantum microscopy

AVS Quantum Science **4**, 034404 (2022); <https://doi.org/10.1116/5.0114436>






## Instruments for Advanced Science

- Knowledge,
- Experience,
- Expertise


Click to view our product catalogue

Contact Hiden Analytical for further details:  
[www.HidenAnalytical.com](http://www.HidenAnalytical.com)  
[info@hideninc.com](mailto:info@hideninc.com)




Gas Analysis

- ▶ dynamic measurement of reaction gas streams
- ▶ catalysis and thermal analysis
- ▶ molecular beam studies
- ▶ dissolved species probes
- ▶ fermentation, environmental and ecological studies




Surface Science

- ▶ UHVTPD
- ▶ SIMS
- ▶ end point detection in ion beam etch
- ▶ elemental imaging - surface mapping



Plasma Diagnostics

- ▶ plasma source characterization
- ▶ etch and deposition process reaction kinetic studies
- ▶ analysis of neutral and radical species



Vacuum Analysis

- ▶ partial pressure measurement and control of process gases
- ▶ reactive sputter process control
- ▶ vacuum diagnostics
- ▶ vacuum coating process monitoring



# Combined ultraviolet- and electron-beam lithography with Micro-Resist-Technology GmbH ma-N1400 resist

Cite as: J. Vac. Sci. Technol. B 40, 052603 (2022); doi: 10.1116/6.0001918

Submitted: 15 April 2022 · Accepted: 10 August 2022 ·

Published Online: 23 September 2022



D. J. Thoen,<sup>1,a)</sup> V. Murugesan,<sup>2</sup> A. Pascual Laguna,<sup>2</sup> K. Karatsu,<sup>2</sup> A. Endo,<sup>1</sup> and J. J. A. Baselmans<sup>2</sup>

## AFFILIATIONS

<sup>1</sup>Department of Microelectronics, Faculty of Electrical Engineering, Mathematics and Computer Science, Delft University of Technology, Mekelweg 4, 2628 CD Delft, The Netherlands

<sup>2</sup>SRON Netherlands Institute for Space Research, Niels Bohrweg 4, 2333 CA Leiden, The Netherlands

<sup>a)</sup>Author to whom correspondence should be addressed: [D.J.Thoen@Tudelft.nl](mailto:D.J.Thoen@Tudelft.nl)

## ABSTRACT

We present a “mix-and-match” process to create large structures with submicrometer features by combining UV contact lithography and 100 kV electron-beam lithography in a single layer of negative-tone resist: Micro-Resist-Technology ma-N1405. The resist is successfully applied for the fabrication of an on-chip terahertz spectrometer, where the design requires 450 nm wide lines and 300 nm wide trenches in a 150 nm thick niobium-titanium-nitride layer, tolerating errors of  $\pm 30$  nm. We use a resist thickness of 500 nm, optimized to allow reliable SF<sub>6</sub>/O<sub>2</sub>-based reactive ion etching of structures with 30 nm accuracy. We find that resist requires an electron-beam cross-linking dose of 1100  $\mu\text{C}/\text{cm}^2$  for an acceleration voltage of 100 kV in combination with a 180 s 100 °C bake on a hot plate and 45 s development. The smallest resist bars made with our dedicated recipe are 100 nm wide, with the smallest gaps about 300 nm. The difference between the designed and realized feature size is between 2 and 30 nm for structures up to 700 nm wide. The optical exposure dose is 300 mJ/cm<sup>2</sup> for the same development time and is optimized to produce a positive sloped edge profile allowing good step coverage for subsequent layers. The resist can be applied, shipped, and processed in a time span of a couple of days without notable deterioration of patterning quality.

© 2022 Author(s). All article content, except where otherwise noted, is licensed under a Creative Commons Attribution (CC BY) license (<http://creativecommons.org/licenses/by/4.0/>). <https://doi.org/10.1116/6.0001918>

## I. INTRODUCTION

In the semiconductor industry, the push for smaller feature sizes has resulted in wafer steppers with an increasingly high resolution. However, for many research institutes, state-of-the-art steppers are a nonviable solution due to high costs. Here, optical contact lithography (UV), laser writing, and electron-beam (EB) lithography are typically used. EB lithography provides a high resolution (below 10 nm), high precision and accuracy, and very good overlay accuracy (below 50 nm) without the need for photomask production. It does come at the cost of long writing times, especially for large area exposures. Exposing 50% of the area of a 4 in. wafer can take more than a day.<sup>1</sup> Optical contact lithography is very fast but requires mask plates, and the resolution is limited to features of the order of 1  $\mu\text{m}$ . The overlay accuracy is also of the order of 1  $\mu\text{m}$ . Precision and accuracy can be reduced by occasional

(air)gaps or particles creating interference between mask and resist, which makes it hard to obtain the requested lithographic quality over a full 4 in. wafer. Laser writing systems provide mask-less lithography but with significant writing times as well as minimum feature sizes of the order of 0.5  $\mu\text{m}$  and an overlay accuracy of about 20 nm. For many applications, the combination of large area exposure and high resolution is, therefore, not easily achieved without the use of high-end steppers.

In this paper, we discuss a method that combines UV- and EB-exposures and subsequent development of Micro-Resist-Technology GmbH ma-N1400 resist to create large area exposures in combination with high resolution and small dimensions, following up on pioneering work by Péron *et al.*<sup>2</sup> Our use case is the realization of the DESHIMA 2.0 on-chip spectrometer for sub-mm astronomy.<sup>3</sup> This device is the successor of DESHIMA, which was recently tested on the ASTE telescope.<sup>4</sup>

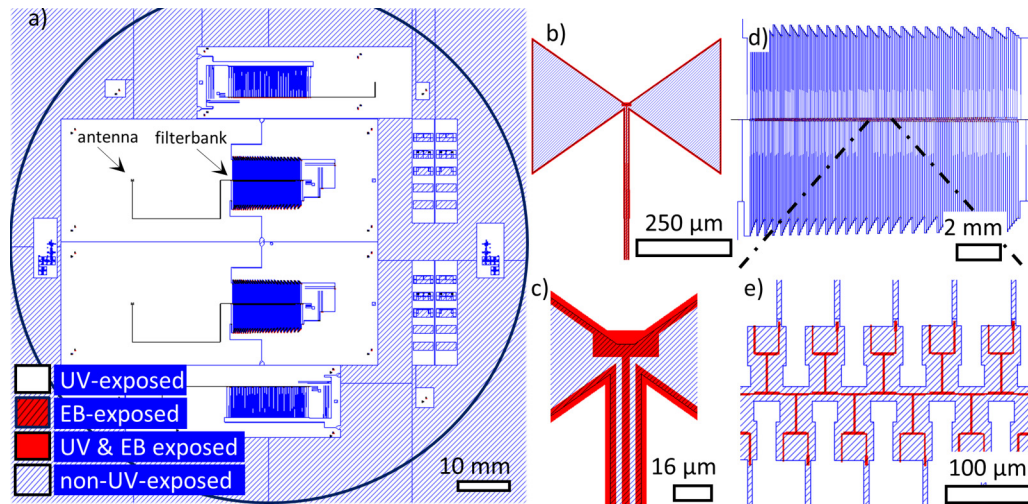


**FIG. 1.** Mask design of a DESHIMA 2.0 spectrometer detector chip, highlighting the NbTiN patterns for mixed EB/UV exposure. The blue dashed color shows non-UV-exposed areas, while white shows the “bright field” or UV-exposed patterns. In red with blue dash, the EB patterns are shown, while areas with both UV and EB exposure are highlighted in red. These double exposed areas are effectively overexposed but have not given notable patterning issues, while the overlap area allows for adequate tolerance for misalignment. (a) Overview of the whole mask. The black circle has a diameter of 100 mm. The biggest chips measure  $62 \times 24 \text{ mm}^2$ . The longest parts of the EB pattern are the narrow lines between the antenna and the filterbank. (b) and (c) Zoom-in on the antenna area (b) and the central part of the antenna (c) showing in red the overlap for EB and UV-exposed parts. (d) and (e) Zoom-in on the patterns of the filterbank.

For this application, we need 450 nm lines separated by 300 nm wide trenches with a maximum variation of  $\pm 30 \text{ nm}$ , etched in a 150 nm thick layer of NbTiN.<sup>5</sup> We need such precise definitions of the line and gap features to limit scatter in the filter frequencies and bandwidths.<sup>6</sup> Additionally, we require positive slopes in the etched NbTiN, especially on the UV-exposed parts, to allow for step coverage by the 40 nm aluminum film, which is deposited in the next processing step. At the same time, the longest lines made with EB lithography have lengths of multiple centimeters, as is clearly visible in the schematic overview of a DESHIMA 2.0 chip design as shown in Fig. 1. The alignment between the UV and e-beam step is not critical: We need a 2  $\mu\text{m}$  alignment accuracy between these two steps.

For our design, a negative resist is preferred over a positive resist in order to limit the EB writing times. However, as can be seen in Fig. 1, the design requires large areas of unetched NbTiN, which implies very long writing times using EB exposure: we estimate a writing time of about 90 h.<sup>1</sup> In this paper, we propose a fast and efficient solution: We expose ma-N1405 negative resist in two steps: 365 nm radiation using a contact mask aligner and 100 keV electrons using an electron-beam system. Both exposure steps are aligned on predefined markers and are followed by a single development and an etching step to create the pattern given in Figs. 2(d)–2(f). This method provides fast and flexible fabrication of large area structures with high-resolution features without the use of expensive steppers.

This paper is structured in the following manner. First, we will discuss the motivation for the use of ma-N1400 and present the procedures we followed to find the boundary conditions and work space for the resist as well as the results of general resolution tests.

In Sec. VI, we will show the final results of full-chip processing of a typical DESHIMA 2.0-spectrometer chip, incorporating the combined optical/electron-beam exposure for patterning the filterbank. We conclude with a discussion and conclusion. We show the EB pattern preparations in the Appendix.

## II. MATERIALS AND EQUIPMENT

All our processing is conducted on 100 mm diameter silicon substrates. Device wafers are 350  $\mu\text{m}$  thick, double-side polished, float-zone-grown intrinsic silicon wafers with  $\rho > 10 \text{ k}\Omega \text{ cm}$ . Since the resistivity is not critical for this work, we use (much cheaper) 525  $\mu\text{m}$ , single-side polished wafers with  $\rho = 1\text{--}10 \text{ }\Omega \text{ cm}$  for process development. The hardware for optical lithography is a SÜSS Micro Tec MJB-6 mask aligner, located at SRON in Leiden, the Netherlands, which uses a 365 nm wavelength mercury source with a GH-line broadband filter for exposure. For the electron-beam exposure, we have a RAITH PG5000Plus-series and a RAITH PG5200 electron-beam pattern generator at our disposal in the Kavli Nanolab of the TU Delft, Delft, the Netherlands. Both systems are operating at a writing speed of 120 MHz with a 100 kV patterning configuration. Reactive ion etching (RIE) is performed with a CORIAL system at SRON or LEYBOLD and SENTECH systems at Kavli. The etchers exploit SF<sub>6</sub>- and O<sub>2</sub>-gas and have similar etching performance and results, making them interchangeable from a processing perspective. Scanning electron microscopy (SEM) is performed with Hitachi Regulus 8230 and Hitachi S4800. The Regulus SEM allows for a secondary electron resolution of 0.7 nm at 1 kV. SEM images are analyzed with ProSEM (GenIsys GmbH), which allows for automated feature size measurements.

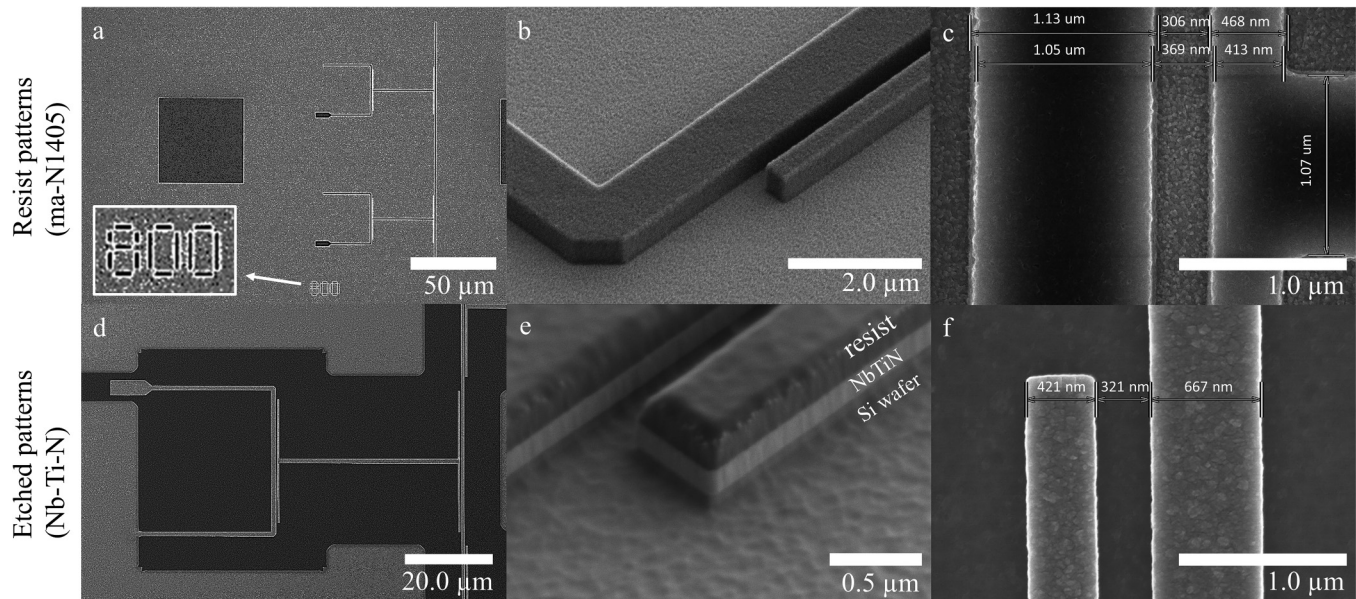


**FIG. 2.** (a)–(c): Micrographs of electron-beam exposed patterns, shortly after resist development. To prevent charging during SEM inspection, the resist is coated with a 10 nm thick sputtered layer of AlSi (1%)-electrolyte. (a) Top view of a unit cell of the EB dose-test pattern, consisting of (1) a square of  $50 \times 50 \mu\text{m}$  (left), (2) a line structure with dimensions comparable to the required structures (right), and (3) an indication of the EB dose (see the inset),  $800 \mu\text{C}/\text{cm}^2$  in this case. (b) Micrograph of the resist line pattern, showing one of the corners of the U-shaped part of the line pattern of the filter as shown in (a). The slope of the resist is very steep, almost  $90^\circ$ . (c) Micrograph of the T-piece corner of the U-shaped pattern. The width at the bottom of the resist patterns is close to the design values. From left to right: 1000 nm wide line (actual +30 nm), a 300 nm wide gap (actual +6 nm), a 450 nm wide line (+18 nm), and a 1000 nm wide central line (+30 nm). The patterns in (b) and (c) are written with an EB dose of  $1600 \mu\text{C}/\text{cm}^2$ . (d)–(f) Micrographs of etched NbTiN features. (d) Zoom-in on a THz-resonator structure pattern created with combined EB and UV exposure. The resist is removed. (e) The micrograph shows a tilted zoom-in on an etched THz-resonator structure pattern similar to Fig. 2(b), with the resist still on top. The slopes of the ma-N1405 resist are rounded, but the sidewall of the NbTiN is very steep, allowing for a high quality pattern definition. An overetch of about 100 nm deep in the crystalline Si of the substrate is visible, as is some underetch under the NbTiN. The NbTiN for this particular test is 210 nm thick. (f) Top-view micrograph of 150 nm thick NbTiN coupler structures on a device wafer fabrication run. Line and gap widths are close to design values: Lines are 20–30 nm narrower than designed. The gap is about 20 nm wider than design. The surface of the patterned NbTiN conformally follows the morphology of the underlying a-Si layer. Magnification is  $50\,000\times$ , and standard deviation is 2.9 nm.

The standard deviation depends linearly on the magnification as well as the finite slope of the sidewall.

### III. RESIST SELECTION

As discussed, a negative-tone, mix-and-match resist is the obvious choice for our application. We have considered two resists from Micro-Resist-Technology GmbH<sup>7</sup> (Germany): the ma-N1400-series<sup>8</sup> and the ma-N2400-series<sup>9</sup> resists. The ma-N2400-series resist is capable of EB and UV-lithography. However, it is discarded for our project as the UV-sensitivity is very low for the 365 nm wavelength source from our mask aligner. The ma-N1400 series resist is marketed as a photoresist but is known to be sensitive for an electron beam as well.<sup>10</sup> Furthermore, the same research showed that it is possible to obtain feature sizes down to 70 nm, which fulfills our requirements. The ma-N1400-series resist can be obtained in multiple dilutions, of which we initially tested ma-N1410 and ma-N1405. The latter can be spun to thicknesses, which match our RIE etch; therefore, the ma-N1405 is the resist that is used throughout this paper.

The EB patterning has the most stringent requirements on the dimensions; therefore, we focus on the EB application parameters and, subsequently, optimize optical lithography. One consideration is that a thinner resist gives a higher resolution and requires less development time. The latter is important as we found that long development times cause an undercut for the resist areas exposed with UV. This is expected from the product sheet<sup>8</sup> and the resist processing guide.<sup>11</sup> Such an undercut is undesirable as we need to ensure good step coverage for subsequent layers deposited after NbTiN patterning.<sup>12</sup> This requires a slightly nonvertical slope of the NbTiN after etching. Hence, we use an RIE plasma with a  $\text{SF}_6$  and  $\text{O}_2$  mixture where the  $\text{O}_2$  erodes the resist while etching, resulting in a sloped edge of the NbTiN. We use a forward power of 50 W, 13.5 sccm  $\text{SF}_6$ , 25 sccm  $\text{O}_2$ , at 0.667 Pa, with typically 1–4 W reflected power and a bias-voltage of 250–300 V.

With aforementioned settings for the etch plasma, we find an etch rate of 2.17 nm/s for the ma-N1405 resist vs 1.17 nm/s for NbTiN, an approximate ratio of 2:1. Hence, a 500 nm thick ma-N1405 resist layer is sufficient to etch 150 nm NbTiN. We obtain a resist thickness of  $493 \text{ nm} \pm 5 \text{ nm}$  when spinning at 3000 RPM for 55 s.

## IV. PROCESS DEVELOPMENT

### A. Resist baking, dose, and development

We bake this resist prior to exposure at 100 °C on a hot plate, as advised in the ma-N1400 product sheet<sup>8</sup> and processing guidelines.<sup>11</sup> However, we use a baking time of 3 min instead of 60 s to minimize contamination of the electron-beam pattern generator (EBPG) system by resist outgassing.

The prescribed development time for the ma-N1405 resist is 18 s, in combination with a 250 mJ/cm<sup>2</sup> UV dose.<sup>8</sup> The initial test showed that this development time is insufficient to remove all unexposed resists after e-beam exposure. This could potentially be the result of a low parasitic exposure created by backscattered electrons. We found that a development time of 45 s results in precise and reproducible, steep EB resist patterns as shown in Fig. 4. Longer times do not deteriorate the patterns by much, but this would become even more problematic for the UV optimization as we will discuss below.

In Ref. 10, the e-beam exposure is conducted with a maximum acceleration voltage of 50 kV. We are using a 100 kV acceleration voltage with a 31 nm spotsize, 30 nA current, and a 300 μm final aperture, requiring dose-tests for which we use the patterns as shown in Fig. 2(a). One unit cell contains (1) a large square of 50 μm × 50 μm and (2) representative structures with dimensions comparable to the final design, with lines of 450 nm wide and gaps of 300 nm wide. The unit cells are patterned in an array on a test wafer and are exposed with an increasing dose: 200–2200 μC/cm<sup>2</sup> in steps of 20 μC/cm<sup>2</sup>. The text describing the dose is also part of the pattern in a unit cell. After development, the heights of the squares are measured with a DEKTAK surface profiler. In Fig. 3, we plot the resulting dose curve: the ratio of the

measured thickness ( $T$ ) to the nominal thickness ( $T_0$ ), with a measured average value of 493 nm. From this result, we estimate contrast factor<sup>13,14</sup>  $\gamma = 1.66$  from the 0%–90% thickness range, with doses of, respectively, 200 μC/cm<sup>2</sup> and 800 μC/cm<sup>2</sup>. The contrast factor serves as an input parameter in TRACER software, allowing us to create a “proximity effect correction point spread function” (PEC PSF): for more details, we refer to the Appendix.

From Fig. 3, it is apparent that a “large area” base dose of 1000–1100 μC/cm<sup>2</sup> gives a fully exposed resist, and as a result, we find good patterning results with this dose. The “small structure” dose is higher and is (automatically) calculated using the PEC PSF.

The 45 s development time required for the e-beam exposure results in an undercut in the resist when exposed with the recommended UV dose of 250 mJ/cm<sup>2</sup>. We found that an UV dose of 300 mJ/cm<sup>2</sup> is adequate to prevent undercuts. This dose even results in a moderately steep sidewall slope.

The optimization results in the following final process, used throughout the paper: 3 min baking on a 100 °C hot plate and 45 s development time in MA-D533s (an aqueous-alkaline and a surfactant containing TMAH based developer), stopping the development by rinsing in a de-ionized water of >14 MΩ cm resistivity. UV exposure is done with a dose of 300 mJ/cm<sup>2</sup> for the 365-nm line and an EB large area cross-linking dose of 1100 μC/cm<sup>2</sup> for an 100 kV electron beam. We find that the optically exposed parts have a resist sidewall slope of about 45°, see Fig. 4, which allows for easy and reliable step coverage of later deposited layers. The EB exposed parts show steep slopes of about 85°, see Figs. 2 and 4, which will also allow for step coverage when the deposition of the next layer has an isotropic component, typically the case for sputter deposition.

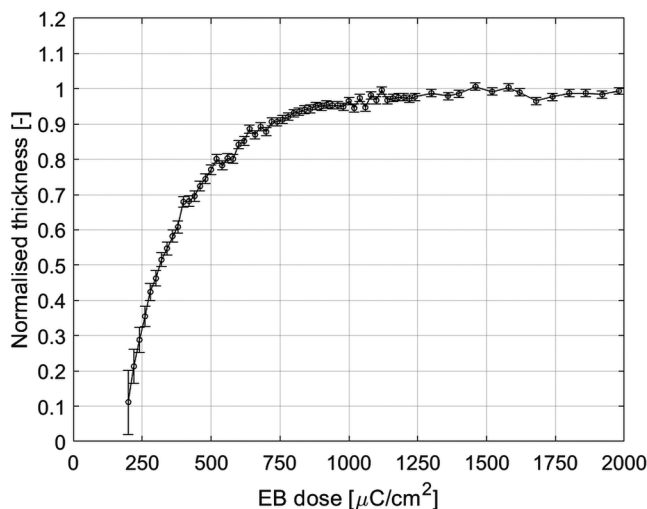


**FIG. 3.** Electron-beam contrast plot of an ma-N1405 resist for 100 kV exposures. The normalized resist thickness of the squares [see Fig. 2(a)] is plotted as a function of their respective dose. Contrast factor  $\gamma$  is 1.66 (Ref. 13) and calculated from the slope at the 0%–90% range. The error bars are 5 nm.

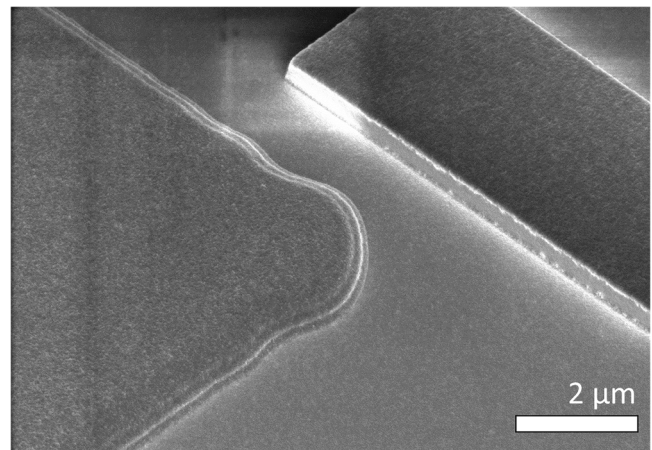


**FIG. 4.** Micrograph of the resist after combined exposure, tilted at 45° from orthogonal, with an UV-exposed pattern on the left and an EB-exposed pattern on the right. The slope of the UV-exposed pattern is positive and moderately steep with about 45° from horizontal: this allows for easy step coverage of subsequent deposited layers. The thickness of the optical exposed resist is about 30 nm thinner than the EB exposed parts.

## B. Electron-beam pattern preparation

Preparation of the EB patterns is given additional attention, as this greatly influences the final quality of the patterns. In the [Appendix](#), we give a full overview of the programs, settings, and calculations used to prepare a pattern. Many considerations are to be taken into account, but a few stand out, which we will shortly discuss. An important artifact is called proximity effect, where the incoming electrons backscatter on the wafer atoms and expose the resist over an extended area, which can result in relatively too low doses for small isolated areas and relatively high doses for large or dense areas. We use TRACER to calculate a PSF in combination with LAYOUT BEAMER (LB), both products of GenISys GmbH,<sup>15</sup> to compensate proximity effects. When performing dose-testing, we do not apply a PEC, where we do apply it when device patterning. The PEC is calculated as a scaling factor with values typically between 0.5 and 2. The base dose is multiplied with this factor to ensure the appropriate dose for both fine and coarse features.

The exposure time required for a given area can be calculated via a simple calculation:<sup>1</sup> (exposure time) = (exposed area) × (resist sensitivity)/(EB current). The smallest possible exposure time is defined by the system blanking speed at 120 MHz or about 8.33 ns. For a very small exposed area, the current has to be reduced to prevent exceeding the blanking speed, which leads to relatively longer writing times for a very small resolution. Details, such as resolution, writing grid, dose, PEC, processing bias, EB current, and beam size, have to be carefully assessed during pattern preparation to ensure minimal writing time and adequate patterning quality.

## C. Stability of resist

For our device wafers, we will combine cleanroom work in two different laboratories (SRON Leiden and Kavli Delft), involving nonconditioned shipment. Typically, our route spans a couple of days from resist spinning, exposures, development, etching to removal of resist. The resist and its consecutive patterning performance should be stable for these uncontrolled time scales and conditions. Initially, we tested the stability by spinning and baking resist on day one, EB exposure on day three, and optical exposure and development at day seven. During this time, the wafer stayed in the same, conditioned environment of the cleanroom. Samples are packed in an aluminum foil to prevent unwanted exposure. We did not observe any deviation in the quality of the resist or patterning. The second part of this trial has been to ship exposed device wafers from lab “A” to lab “B”: we have not observed negative effects on the patterning quality. During transport, the wafers are stored in optically tight single wafer boxes, wrapped in an aluminum foil, and double packed in dust-free ESD-safe seal bags. We learned that the resist is sufficiently stable during unconditioned transport while processing is spread over a week.

## V. FINAL RECIPE

In [Fig. 5](#), we show the resulting resist profiles of the final recipe as discussed in [Sec. IV](#). We are able to create resist lines down to 100 nm in design width, while the 50 nm wide line has fallen over despite the use of PEC and a 15 nm processing bias

compensation. The increasing error for small line features points at a lack of dose, while the wider lines show overdose effects. Trenches of 200 nm and narrower are underdeveloped and show parasitic exposure. This points at the PEC having a unbalanced effect for varying widths. Tuning of the PEC point spread function is expected to allow for compensation and reduction of the error in width.

In [Fig. 6](#), we present the result of a combined optical and e-beam exposure, development and etch of a 150 nm thick NbTiN film. Both EB and UV patterns are aligned on optically patterned markers on the wafer, and we find an alignment accuracy of  $\pm 1 \mu\text{m}$ . SEM inspection is followed by analysis with ProSEM. The width of the narrow lines is about 30 nm less than designed, and the trench is about 30 nm wider, with a standard deviation of 2.9 nm at a magnification of 50 000×. The final dimensions of the patterns are a convolution of the age and application details of the resist, the applied base dose, and PEC settings (for EB) as well as the processing bias. We have observed that the ma-N1400 resist older than the expected storage life becomes less sensitive. For the device wafer fabrication, we can apply a processing bias correction in the LB as a first order correction to the observed processing bias: We broaden the lines 15 nm per side, resulting in 30 nm wider lines while narrowing the trenches with the same amount.

## VI. DEVICE WAFER FABRICATION

We have used the process discussed in this paper to pattern the top NbTiN layer in the fabrication of the next-generation on-chip spectrometer DESHIMA 2.0.<sup>6</sup> A micrograph of the resulting microstrip filter-bank on-chip spectrometer is shown in [Fig. 7](#), and the full fabrication details are given in [Ref. 16](#). Markers for the EB and UV alignment are created in the bottom NbTiN layer (layer 2) in this process.

## VII. DISCUSSION AND CONCLUSION

We have successfully developed a method to perform mix-and-match patterning of ma-N1405 resist. A single layer of resist is exposed with both an electron beam and optical lithography, followed by a single development. For a 500 nm thick ma-N1405 resist layer baked for 3 min at 100 °C on a hot plate and a 45 s development in MA-D533s, we found a large area EB cross-linking dose of 1100  $\mu\text{C}/\text{cm}^2$  and a 300  $\text{mJ}/\text{cm}^2$  optical exposure to give properly shaped and developed patterns. For EB, we found a contrast factor of  $\gamma = 1.66$  with the following beam settings: 100 kV acceleration voltage, 31 nm spotsize, 30 nA current, and 300  $\mu\text{m}$  final aperture.

The EB exposed patterns have a very sharp definition, and we can write solitary resist lines down to 100 nm in width and gaps of 300 nm wide, both limited by the thickness of the resist. The error in the dimensions of the etch patterns is about 30 nm. The sidewalls are very steep, approximately 85°. The optically exposed parts of the resist show an edge slope steepness of about 45°, which is excellent for a step coverage of subsequent deposited layers.

Once baked, the resist is very stable over time: we did not observe degradation of the patterning quality for processing with seven days of space between baking and development, neither for

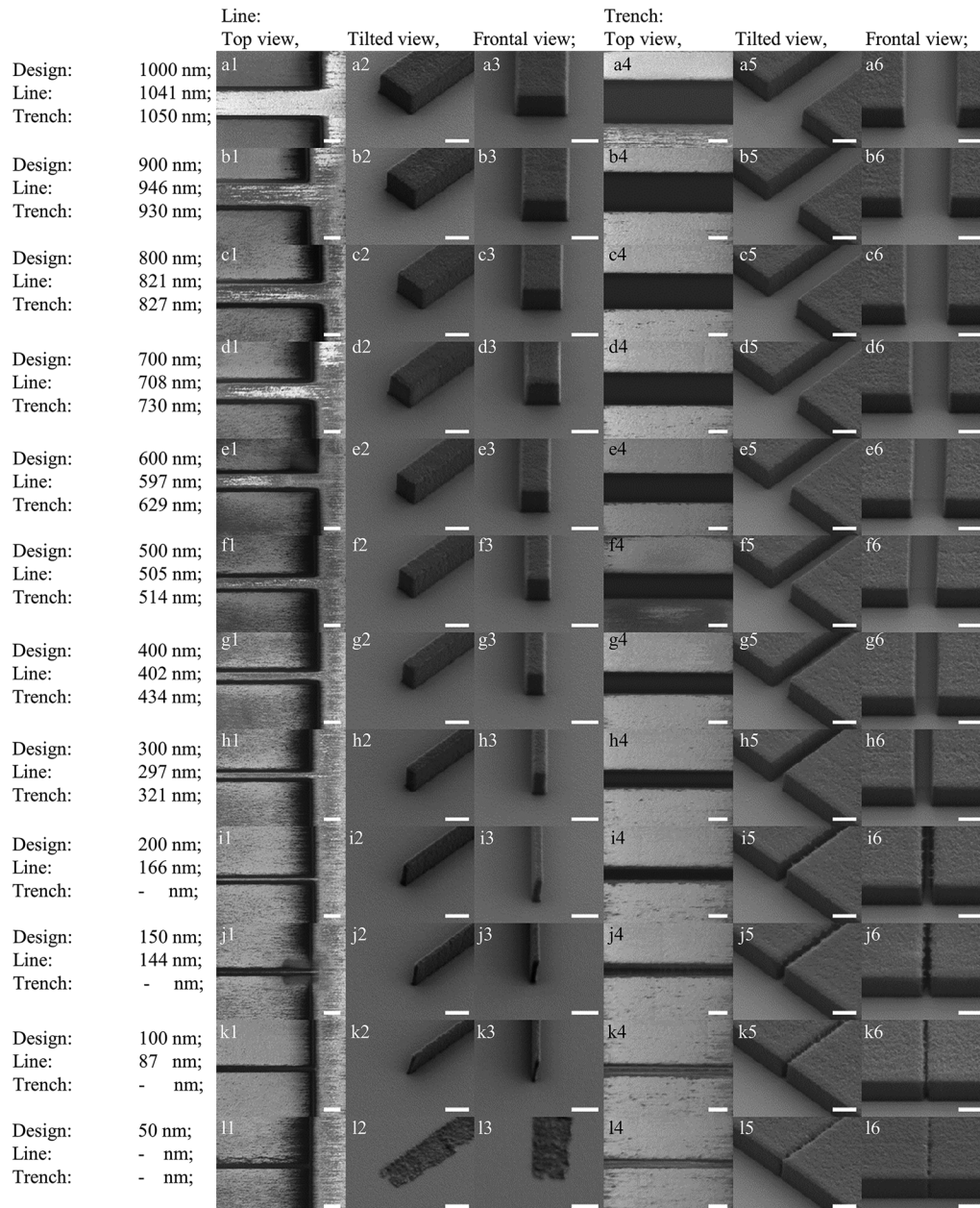


**FIG. 5.** Micrographs of patterned resist structures fabricated with settings as used for our final fabrication route. Columns: (1)–(3): line patterns and (4)–(6): patterns of trench features. Rows (a)–(l) depict varying design widths. The scale bar has a reference 500 nm length. There is no electrolyte on the resist. The width of the structures is determined with ProSEM and has a standard deviation of 5 nm at 30 000 $\times$  magnification. The 50 nm line has toppled over. Trenches of 200 nm and smaller are underdeveloped. We expect that creating smaller structures can be achieved by tuning the combination of resist thickness, processing bias correction, exposure dose, and development time.

processing in multiple labs, including unconditioned shipment to and from the respective laboratory.

Selectivity for SF<sub>6</sub>/O<sub>2</sub> RIE etching of the resist is a factor of 0.5, requiring a resist at least twice thicker than the

thickness of the NbTiN being etched. The slopes of the EB exposed NbTiN patterns remain very steep, approximately 85°. At the same time, with optical exposure, we can independently create a NbTiN sidewall slope of about 45°,



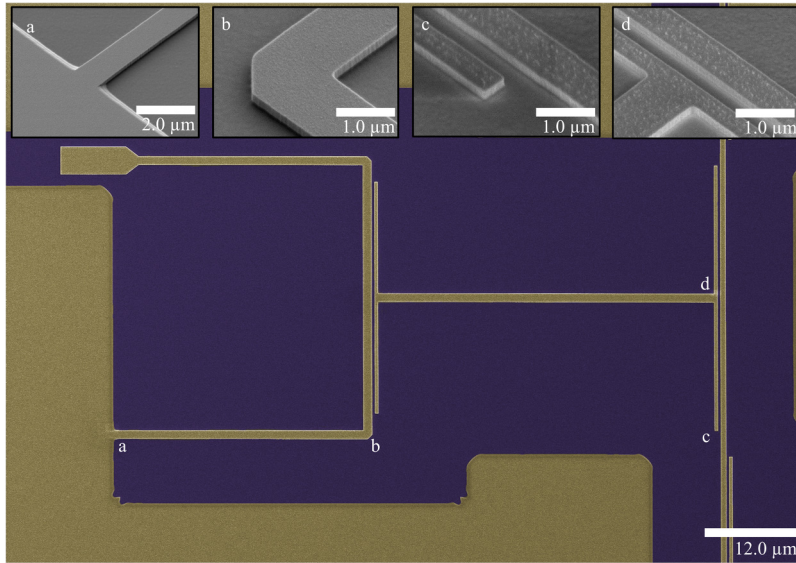


**FIG. 6.** Artificially colored top-view micrograph of an etched NbTiN THz-filter element (golden) on Si (purple). The optically exposed NbTiN suffers from lithographic distortions clearly visible at the corner rounding. The insets (a)–(d) refer to the respective parts of the etched pattern where we zoom in. (a) Seamless overlap of optical and EB exposed parts of the pattern. The optically exposed NbTiN shows a edge slope steepness of about  $45^\circ$ , where EB exposed structures show almost vertical slopes. (b) Isotropic etching of the c-Si creates an undercut under NbTiN. (c) and (d) High-resolution EB structures of NbTiN on a-Si. The lines are well patterned and are typically 30 nm narrower than designed, and the gaps are approximately 30–40 nm wider than designed.

which allows an easy and reliable step coverage for later deposited layers.

The excellent performance of the resist allows us to minimize writing time of large areas and coarse features (features  $<2\mu\text{m}$ , while enabling high-resolution lithography where required. For the on-chip integrated filterbank structures, we can reliably and

reproducibly make 450 nm wide lines and 300 nm wide trenches, with a tolerance of about 30 nm. The EB writing time is about 30 min for a 6.25 nm beam step size. Further fine tuning of the PEC point spread function and processing bias correction will allow for smaller errors. Interestingly, we estimate a writing time of 90 h with the largest current and beam if we would use EB exposure for the area that is now exposed with UV in a matter of seconds. We have fabricated a first version of the next-generation on-chip THz integrated filterbank of DESHIMA 2.0, with 100% fabrication yield.

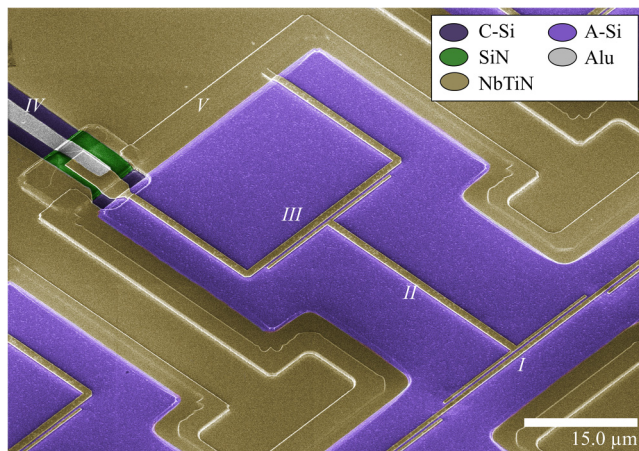


**FIG. 7.** Overview of parts of a finished microstrip filter-bank on-chip spectrometer chip, exploiting combined optical and electron-beam lithography for patterning the NbTiN filter-bank layer. The 700 nm wide THz signal-line (I) runs diagonally from the center bottom to the right side, capacitively coupling the signal in the THz-filter (II). The THz-filter is read out by a microwave kinetic inductance detector, of which the hanger part (III) is visible, which connects to the Al-part (IV) at the top left and shorts to the ground plane on the other side (V). In this case, the Al-NbTiN step coverage is facilitated by an SiN patch. Later versions lack this SiN patch, which is replaced by polyimide.

## ACKNOWLEDGMENTS

The authors want to express their gratitude to Ing. Anja van Langen-Suurling of Kavli Nanolab Delft for discussion and assistance for the EBPG and to the staff of the SRON cleanroom. The contribution of J.J.A. Baselmans was supported by the ERC CoG 648135 MOSAIC.

## AUTHOR DECLARATIONS

### Conflict of Interest

The authors have no conflicts to disclose.

## Author Contributions

**D. J. Thoen:** Data curation (lead); Formal analysis (equal); Investigation (equal); Methodology (lead); Resources (equal); Validation (equal); Visualization (equal); Writing – original draft (lead); Writing – review & editing (lead). **V. Murugesan:** Data curation (equal); Formal analysis (equal); Investigation (lead); Methodology (supporting); Resources (equal); Validation (equal); Writing – original draft (supporting). **A. Pascual Laguna:** Conceptualization (supporting); Formal analysis (supporting); Investigation (supporting); Writing – original draft (supporting);

Writing – review & editing (supporting). **K. Karatsu:** Conceptualization (supporting); Data curation (supporting); Resources (supporting); Writing – original draft (supporting). **A. Endo:** Conceptualization (lead); Formal analysis (equal); Funding acquisition (equal); Investigation (equal); Project administration (equal); Supervision (lead); Writing – original draft (supporting). **J. J. A. Baselmans:** Conceptualization (lead); Funding acquisition (lead); Investigation (equal); Project administration (equal); Supervision (lead); Writing – original draft (equal); Writing – review & editing (equal).

#### DATA AVAILABILITY

The data that support the findings of this study are available from the corresponding author upon reasonable request.

#### APPENDIX: PATTERN PREPARATION FOR ELECTRON-BEAM EXPOSURES

Pattern generation for EB is performed in multiple steps (see Fig. 8):

- Mask creation: Creation of the mask files by any commercial CAD program, such as AutoCAD, CleWin, or others.
- CAD preparation: This involves commercial TRACER and LB software packages (GenlSys GmbH, Germany). EB patterning suffers from energy distributed outside the scanned pattern, caused by scattering of the incoming electrons. It is commonly

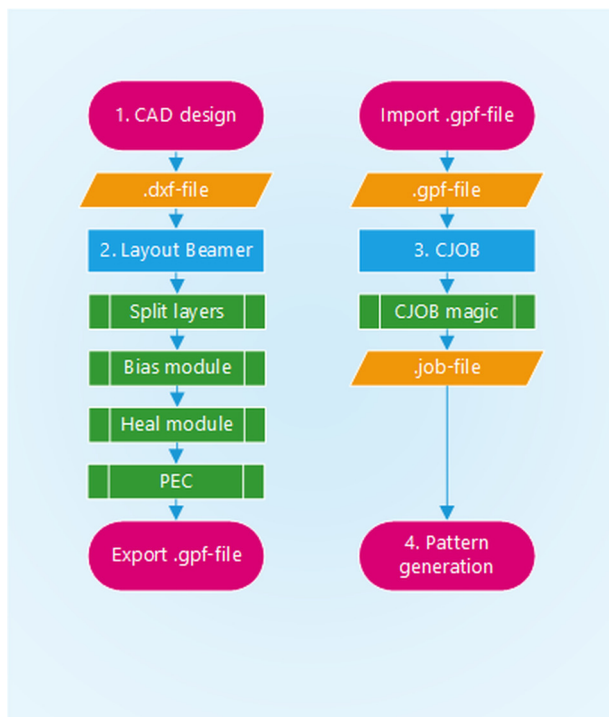


FIG. 8. Flow chart for electron-beam pattern preparation.

referred to as a proximity effect and typically results in overexposure of relative large patterns and underexposure of relatively small patterns. The proximity effect is systematic and can be mitigated with the aforementioned software packages. TRACER performs Monte-Carlo calculations to predict the systematic variations in the EB dose based on the electron-beam current settings, and the materials and thicknesses of the layers of the device stack are exposed. The results are used as an input for the PEC module in LB. LB (v5.8) creates a point spread function based on the mask files and also contains a module to apply the PEC. A .gpf-file is created and exported for step 3.

- Pattern generator preparation: importing of the .gpf-files in the pattern generator, creating a .job-file using the CJOB-program (Raith). With CJOB, it is possible to organize the alignment of the .gpf-mask files with markers on the wafers and choose a cross-linking dose, beam, and add support text or structures to the job to be written.
- Electron-beam patterning: Actual writing of the pattern, using a .JOB-file.

The following modules are used in LB: Import, Extract, Transform, Size, Heal, PEC, and Save (export). Below, we give an overview of typical settings.

- Import dxf file: We read the .dxf file and set the Database Grid at a fixed value of 0.001  $\mu\text{m}$ .
- Extract layers: We select the layer(s) of interest.
- Transformation: Rotate the patterns  $-90^\circ$  to align the pattern with the wafer holder at the EBPG.
- Pattern bias: Apply a bias to the patterns: We enlarge the structures by 15 nm to counteract the processing bias. The bias is  $n$  times the BSS 6.25 nm in our case) and depends on process bias parameters.
- Apply healing: The healing process mode removes all overlap and flattens the layer.
- Proximity effect correction: This module calculates a spatially varying dose depending on the pattern size and density and device and beam characteristics to prevent over- or underexposure of features. We apply a numerical point spread function as calculated by TRACER, with an Effective Short Range Blur (FWHM) of 10 nm, add Gamma (0.001  $\mu\text{m}$ ) and Nue [0.1 (unitless)], and include the short range correction. Lateral development correction is not used since we already compensated this effect in size. Other settings are unaltered.
- Save the file: Format type: 5200/5000+ 20 bit HS 100 kV v1.43 (UPG), with a resolution (and a beam step size) of 6.25 nm. The mainfield resolution is 1/10 of BSS: 6.25 nm, and the subfield resolution is 1/20 of BSS: 0.3125 nm. We apply an “LRFT” fracturing mode and a high-resolution fracture control and export a .gpf-file.

TRACER: Our pattern and resist optimization is based on GenlSys Application Notes. The large structure cross-linking dose is the first parameter that we need and is obtained from an EB-dose test of the resist, with both large and small structures [see Fig. 2(a)] and without using PEC.

## REFERENCES

- <sup>1</sup>N. W. Parker, A. D. Brodie, and J. H. McCoy, *Proc. SPIE* **3997**, 713 (2000).
- <sup>2</sup>I. Péron, P. Pasturel, and K. F. Schuster, *IEEE Trans. Appl. Supercond.* **11**, 377 (2001).
- <sup>3</sup>A. Taniguchi *et al.*, “DESHIMA 2.0: Development of an integrated superconducting spectrometer for science-grade astronomical observations,” [arXiv:2110.14656](https://arxiv.org/abs/2110.14656).
- <sup>4</sup>A. Endo *et al.*, *Nat. Astron.* **3**, 989 (2019), [arXiv:1906.10216](https://arxiv.org/abs/1906.10216).
- <sup>5</sup>D. J. Thoen, B. G. C. Bos, E. A. F. Haalebos, T. M. Klapwijk, J. J. A. Baselmans, and A. Endo, *IEEE Trans. Appl. Supercond.* **27**, 1500505 (2017).
- <sup>6</sup>A. Pascual Laguna, K. Karatsu, D. J. Thoen, V. Murugesan, B. T. Buijtdorp, A. Endo, and J. J. A. Baselmans, *IEEE Trans. Terahertz Sci. Technol.* **11**, 635 (2021).
- <sup>7</sup>Micro-Resist-Technology GmbH, “Homepage,” (2021); see: <https://www.microresist.de/>; accessed 24 August 2021.
- <sup>8</sup>Micro-Resist-Technology GmbH, “ma-N1400 product sheet,” (2021); see: [https://www.microresist.de/en/?jet\\_download=2437](https://www.microresist.de/en/?jet_download=2437); accessed 24 August 2021.
- <sup>9</sup>Micro-Resist-Technology GmbH, “ma-N2400 product sheet,” (2021); see: [https://www.microresist.de/en/?jet\\_download=2432](https://www.microresist.de/en/?jet_download=2432); accessed 24 August 2021.
- <sup>10</sup>A. Aassime and V. Mathet, *J. Vac. Sci. Technol. B* **27**, 28 (2009).
- <sup>11</sup>Micro-Resist-Technology GmbH, “Processing guidelines PG\_ma-N1400\_2015,” private communication (30 November 2018).
- <sup>12</sup>L. Ferrari *et al.*, *IEEE Trans. Terahertz Sci. Technol.* **8**, 127 (2018).
- <sup>13</sup>R. A. Pethrick, *Int. J. Radiat. Appl. Instrum. Part C* **37**, 331 (1991).
- <sup>14</sup>A. Gangnaik, Y. Georgiev, and J. Holmes, *Chem. Mater.* **29**, 1898 (2017).
- <sup>15</sup>GenISys GmbH, “Homepage,” (2021); see: <https://www.genisys-gmbh.com/>; accessed 24 August 2021.
- <sup>16</sup>A. Pascual Laguna, “On-chip solutions for future THz imaging spectrometers,” Ph.D. thesis (Delft University of Technology, 2022).